The Effect of Noise in Computed Tomographic Reconstructions on Detectability

Kenneth M. Hanson
University of California
Los Alamos National Laboratory
Los Alamos, New Mexico 87545

Abstract

The detectability of features in an image is ultimately limited by the random fluctuations in density or noise present in that image. The noise in CT reconstructions arising from the statistical fluctuations in the one-dimensional input projection measurements has an unusual character owing to the reconstruction procedure. Such CT image noise differs from the "white" noise normally found in images in its lack of low-frequency components. The noise power spectrum of CT reconstructions can be related to the effective density of x-ray quanta detected in the projection measurements, designated as NEQ (noise-equivalent quanta). The detectability of objects that are somewhat larger than the spatial resolution is directly related to NEQ. Since contrast resolution may be defined in terms of the ability to detect large, low-contrast objects, the measurement of a CT scanner's NEQ may be used to characterize its contrast sensitivity.

*Work performed under the auspices of the U S Department of Energy, under contract no. W7405-ENG-36.

1. INTRODUCTION

The x-ray computed tomographic (CT) scanner has made it possible to detect the presence of lesions of very low contrast (New et al., 1978). This dramatic improvement in detection capability over most conventional forms of x-ray imaging is a result of the following innovations: (1) the noise in the reconstructed CT images is significantly reduced through the use of efficient x-ray detectors and electronic processing, thereby improving the utilization of the radiation dose; (2) the images can be displayed with enhanced contrast, thus overcoming the minimum contrast threshold of the human eye; (3) the CT reconstruction technique almost completely eliminates the superposition of anatomic structures, leading to a reduction of "structural" noise.

It is the random noise in a CT image that ultimately limits the ability of the radiologist to discriminate between two regions of different density. Because of its unpredictable nature, such noise cannot be completely eliminated from the image and will always lead to some uncertainty in the interpretation of the image. There is strong evidence that most of the random noise in present-day CT scanners is due to the statistical inaccuracies arising from the detection of a finite number of transmitted x-ray quanta. The properties of this statistical noise in CT images will be discussed in this article. The goal will be to characterize the noise content in a way that is closely related to the detection capabilities inherent in the image.

It will be shown in the discussion of the optimum receiver that the ability to detect a large-area object in a CT image is chiefly dependent on the NEQ, the total number of noise-equivalent quanta detected per unit length in the projections used to reconstruct that image. As such, it is not the fineness with which the x rays are detected in the projections (related to spatial resolution), but simply the effective total number of detected x rays that influences the large-area contrast sensitivity of the CT reconstruction. For a fixed, large-area contrast sensitivity, then, an increase in spatial resolution does not imply the necessity for higher

dose! NEQ, which characterizes the low-frequency properties of noise in a CT image, can be determined from a CT noise image by measuring the noise-power spectrum. This paper represents a distillation of a chapter prepared for Radiology of the Skin and Brain, Vol. 5 (Hanson, 1981).

2. PROPERTIES OF CT NOISE

The consequences of statistical noise in CT reconstructions have been discussed by numerous authors (Shepp and Logan, 1974; Cho et al., 1975; Tanaka and Iinuma, 1975, 1976; Barrett et al., 1976; Brooks and DiChiro, 1976; Chesler et al., 1977; Hanson, 1977,1979a; Huesman, 1975, 1977; Joseph, 1977, 1978; Hanson and Doyd, 1978; Riederer et al., 1978; Wagner et al., 1979). Several of these authors have pointed out that the process of reconstruction leads to some peculiar characteristics of the noise in CT images. The properties of statistical (quantum) noise in CT reconstructions will be explored in this discussion. Although the precise random noise pattern of any image cannot be predicted *a priori*, it is possible to characterize the average behavior of the noise by a variety of methods. Some of these methods give a complete description of the noise characteristics, such as the noise power spectrum or the noise autocorrelation function, whereas others give only a partial description, such as rms noise. It will develop that the noise fluctuation in one pixel of a CT reconstruction is <u>not</u> independent of the noise fluctuations in other pixels. Rather, the fluctuations in two separate pixels are, on the average, correlated.

The ramplike nature of the noise power spectrum expected for CT reconstructions will be derived for the filtered back projection algorithm. It will be shown that noise power spectra of EMI CT5005 reconstructions possess this ramplike behavior at low frequencies.

Before proceeding, it should be mentioned that the present discussion is concerned only with the random noise that results from the statistical variation in the number of detected x-ray quanta. CT reconstruction may also contain unwanted features that arise from deficiencies in the data collected such as too few views, not enough samples taken in each view (aliasing), beam hardening of the polychromatic x-ray beam, partial volume effects, etc. (Joseph, 1981, Herman, 1979.) These unwanted signals are termed artifacts. They will not change in a series of identical scans since they arise from systematic errors. Artifacts may be arbitrarily reduced by improved scanning and reconstruction procedures. However, statistical noise can only be reduced by increasing the number of detected x rays either through an improvement in x-ray detection efficiency (many of today's scanners are within a factor of two of the most practical efficiencies attainable) or through an increase in patient dose.

2.1 ORIGIN OF IMAGE NOISE

The energy in x-radiation is transmitted in the form of individual chunks of energy called quanta. Hence, the response of an x-ray detector is actually the result of detecting a finite number of x-ray quanta. The number of detected quanta will vary from one measurement to the next, because of statistical fluctuations that naturally arise in the "counting" process. As more quanta are detected in each measurement, the relative accuracy of each measurement improves. Statistical noise in x-ray images arises from the fluctuations inherent in the detection of a finite number of x-ray quanta. Statistical noise may also be called quantum noise and is often referred to as quantum mottle in film radiography.

Statistical noise clearly represents a fundamental limitation in x-ray radiographic processes. The only way to reduce the effects of statistical noise is to increase the number of detected x-ray quanta. Normally this is achieved by increasing the number of transmitted x rays through an increase in dose. Figure 1 shows a series of scans taken on a GE CT/T 7800 scanner* using a phantom designed to test contrast sensitivity. The reduction in the noise caused by increasing the x-ray exposure (milliampere seconds) is graphically demonstrated.

In processing electric signals, electronic circuits inevitably add some noise to the signals. Analog circuits, those which process continuously varying signals, are most susceptible to additional noise. Thus the stage most likely to inject additional electronic noise is that of analog signal processing of the x-ray detector's output. The difficulty of noise suppression is compounded by the fact that for some types of x-ray detectors, the electronic signals are very small. There is evidence (Cohen, 1979) that many commercially

*General Electric Medical System Division, Milwaukee, WI

available CT scanners are sufficiently well engineered to reduce the contribution of electronic noise under normal operating conditions to a fraction of the statistical noise contribution.

2.2 FOURIER ANALYSIS--NOISE POWER SPECTRUM

Any signal may be thought of as a sum of sine waves of appropriate frequency, amplitude, and position (phase). This decomposition of a signal into its frequency components is called Fourier analysis. It is often helpful to apply Fourier analysis to imaging systems (cameras, television, x-ray radiographs, etc.) because of the ease with which the imaging properties of various stages of the systems combine in their frequency representations. To be sure, Fourier analysis is only useful for linear systems, but most imaging techniques are approximately linear for small changes in signal amplitudes. A good introduction to the application of Fourier analysis to radiography may be found in Johns and Cunningham (1969), and to image analysis in Dainty and Shaw (1974).

The noise power spectrum is related to the frequency decomposition of the image noise. The noise power spectrum is often referred to as the Wiener spectrum. Often the response of the system is assumed to be circularly symmetric. Then the two-dimensional noise power spectrum may be reduced to a one-dimensional spectrum that is a function of only the radial frequency (distance from zero frequency in two dimensions).

The noise found in conventional radiographs is typified by a noise power spectrum that is roughly constant over a wide range of frequencies. Such a noise power spectrum is called "white" in analogy to white light, which contains a mixture of light of all frequencies within the visible spectrum. A white noise power spectrum indicates that the random fluctuations at one point in the image is uncorrelated with or independent from fluctuations at another point. In conventional radiographs this comes about since separate x rays are detected at two different points. Thus, the statistical fluctuations giving rise to noise at one point are not related to the fluctuations occuring at a different position. Statements such as this can be made only if the points are separated by a distance sufficiently large to avoid "cross talk" between the points. Consequently, the noise power spectra of all physical systems must eventually fall to zero at high frequencies.

2.3 VISUAL EXAMPLE

The relationship between the noise power spectrum and the noise it characterizes may be displayed visually. Figure 2 shows images containing two types of noise, one typifying white noise, and the other, CT noise. The rms deviation of the noise is the same in both images. The noise power spectra of these images is shown in Fig. 3. White noise, typical of film radiography (see above) is characterized by a flat power spectrum at low frequencies. In this example its power spectrum falls off at intermediate frequencies because of an assumed Gaussian modulation transfer function (MTF), that is, $\exp(-af^2)$. As discussed later, the CT noise power spectrum typically is linear at low frequencies going toward zero at zero frequency. In this example the CT noise power spectrum peaks at midfrequencies and then falls off with the same MTF as the white noise spectrum. The major difference between the two noise power spectra of Fig. 3 is the greatly diminished contribution at low frequencies typical of CT noise. Since low frequency corresponds to large distance, the CT noise image would be expected to have little contribution from clumps of noise with large area. The reduced blotchiness of the CT noise can be seen in Fig. 2, especially when the figure is observed from a distance so the eye is tuned to large-area structure.

2.4 DEPENDENCE ON RECONSTRUCTION ALGORITHM AND NEQ

The noise power spectrum for CT noise has been derived by Riederer et al. (1978). The derivation is based on the filtered back projection algorithm (Shepp and Logan, 1974) for a parallel-beam geometry in which a constant density of x rays is detected in all the projections. The corrective filter applied to the Fourier transforms of the projections is assumed to be

$$G(f) = |f| H(f) , \qquad (1)$$

where f is the frequency, and H is a weighting (or apodization) factor. The principal restriction on H is that it be nearly unity for very low frequencies f. It may be shown that the noise power spectrum S for statistical CT noise can be written as follows (Riederer et al., 1978; Hanson, 1979a; Wagner et al., 1979):

$$S(f) = \frac{|f|^2 H^2(f)}{NEQ} , \qquad (2)$$

where NEQ, the number of noise-equivalent quanta, is the total effective number of x-ray quanta detected per unit distance along the projections (summed over all the projection measurements). If there is no source of noise other than statistical and the reconstruction algorithm is efficient, then NEQ will be just the total number of detected x rays per unit projection length. The presence of other sources of noise can reduce NEQ compared with the actual number of detected quanta. Also, the measurement of the x-ray fluence by means of an energy-integrating detector (as is done on essentially all commercial CT scanners) leads to a slight reduction (~10%) in NEQ compared to that attainable through x-ray counting. In equation 2 it is assumed that the reconstruction image attenuation coefficient is given in units of (cm^{-1}). Then S will be dimensionless and NEQ will have dimension (cm^{-1}), as it should.

Equation 2 indicates that the noise power spectra of CT reconstructions should have a ramplike dependence at low frequencies (where H = 1). The slope of S at low frequencies is determined by NEQ. As such, NEQ may be used to characterize the large-area, low-contrast detection capabilities of CT images (see discussion of optimum receiver). It shall be shown that equation 2 implies there is no loss in detection performance in a filtered back projection reconstruction compared to the input projection data for large objects. As more quanta are detected, S will be reduced inversely and the CT image noise will diminish.

The dependence of S on the weighting factor 'H' of the algorithm should be noted. H may be regarded as the MTF associated with the reconstruction algorithm in the absence of aliasing problems associated with the finite size of the reconstruction pixels (Hanson, 1979b). The MTF of the complete scanner system is the product of all the MTFs that contribute to the spatial resolution of the final image. For many CT scanner systems the dominant contribution is the MTF associated with the finite width of the radiation beam used in the projection measurements (Barnes et al., 1979). Thus, although the total noise of the CT scanner is closely related to the spatial resolution of the reconstruction algorithm, it may have only a weak dependence on the overall spatial resolution. It should also be realized that the image noise is not dependent on the pixel size except insofar as the latter affects the choice of H.

2.5 rms NOISE

Frequently the rms deviation of the noise is quoted for CT reconstructions. It should be clear that the rms noise is not a complete characterization of CT noise, since it ignores the frequency dependence of the noise. Specifically, the rms noise depends critically on the high frequency damping factor H(f) used in the reconstruction algorithm, which will vary from one CT scanner to the next. It will be shown that the ability to detect large-area objects is related to the low-frequency noise power content, which is relatively unaffected by H(f). Thus, detectability is not simply related to the rms noise.

The rms noise may be calculated from the noise power spectrum (by Parseval's theorem) as the square root of the total noise power

$$\sigma = \sqrt{\iint df_x df_y S(f_x, f_y)} = \sqrt{2 \int df\, f\, S(f)}\,. \qquad (3)$$

Since σ^2 is the integral of the noise power spectrum, it contains no information about the frequency dependence of the noise.

2.6 RESULTS FOR A COMMERCIAL SCANNER

The noise power spectrum has been calculated for an EMI CT5005 scanner* to demonstrate that it has the form predicted by equation 2 (Hanson, 1979a). The EMI 26-cm-diameter water calibration phantom was scanned six times at 140 kVp, 28 mA using the normal scan time (20 seconds). The 320 x 320 reconstruction matrix was obtained by decoding the EMI magnetic tape. The pixel size is 0.75 mm. These scans were performed at the University of California (San Francisco) Medical Center in October, 1977, and the scanner was not equipped with the new dose-reducing collimator (EMI 5221).

Analysis of the reconstructions showed that the rms deviation of the noise (1.28%) was constant over the whole image to very good accuracy. Furthermore, the average values in the reconstructions were uniform to better than 0.1%. Figure 4 shows one of the water scans used. Any variations seen in Fig. 4 can arise only from either the display

*EMI Medical Inc., Northbrook, IL

unit or subsequent film processing. The presence of the film-roller mark points out the need for quality control in these often neglected aspects of CT technology.

The noise power spectrum of the EMI reconstructions was calculated in a manner similar to that described in the earlier discussion of noise power spectrum. The resulting spectrum, Fig. 5, has the predicted linear behavior at low frequency (below 0.1 mm^{-1}). The slope of the spectrum at midfrequencies (0.1 to 0.3 mm^{-1}) is greater than at low frequency, indicating that EMI has used a value of H which is greater than 1 at these frequencies. The resulting edge enhancement sharpens edges in the reconstruction to a slight degree. Such edge enhancement is usually accompanied by overshoots and undershoots in the step-response function.

The NEQ of the EMI scans can be obtained from Fig. 5 by using equation 2. The result is NEQ = (1.85 ± 0.03) x 10^7 mm^{-1}. Thus, the total number of equivalent x-ray quanta detected in each scan (product of NEQ times the length of each projection) was 260 mm x 1.85 x 10^7 mm^{-1} = 5 x 10^9!

There are numerous sources of noise other than statistical that may contribute to CT reconstructions. These other noise sources may or may not lead to noise power spectra similar to that expected for statistical noise. However, it has been verified that the noise power spectrum has the expected form for the EMI Mark I by Wagner et al. (1979) as well as for the GE8800 and the Δ2020 by the author.

3. DETECTABILITY IN THE PRESENCE OF CT NOISE

It is clear from Fig. 1 that a reduction in the magnitude of the noise leads to improved detection of contrast differences. But suppose the same phantom were scanned on another scanner with completely different spatial resolution and, more important, a completely different reconstruction algorithm. What measure of noise would allow comparison of the ability to discriminate contrast differences in the two scans? This is the central issue in the description of image noise. It is important to use parameters to characterize the noise that is directly and simply related to detectability. In this discussion the close relationship between NEQ and the detection of large-area objects is described. This relationship is established for the optimum receiver, which fully takes into account the characteristics of CT noise. The connection between the detection performance of the optimum receiver and that of the human observer is not well documented. However, it is expected that the two performances will track each other in a relative evaluation of similar images. Thus the basis of comparison dictated by the optimum receiver will probably be useful in the comparison of clinical images.

3.1 DETECTION TASK

To simplify matters, only the binary decision problem will be considered here. The decision to be made is whether a specific object is present at a specific location. Furthermore, it is assumed that the background on which the object is superimposed is completely specified. This detection problem is exemplified by the phantom in Fig. 1 in which circular objects are present on a flat background. However, the presence of a row of circles rather than a single circle alters the problem slightly and complicates the analysis of the results. The binary decision case may be extended to the multiple decision problem (Goodenough, 1975; Goodenough and Metz, 1974) or to the problem of the search for objects within an image (Wagner, 1977). Although the binary decision problem represents a gross simplification of the clinical detection situation at present this simplification is necessary to permit theoretical analysis and psychophysical testing.

Clinical diagnosis clearly relies heavily on the ability of the radiologist to recognize patterns. The general pattern recognition problem is very difficult to model in full detail. However, the ability to detect component parts of a pattern must form the basis of pattern recognition. Thus, it is hoped and expected that results obtained from analysis of the simple detection problems often encountered in psychophysical testing will be relevant to the more complex clinical situation.

3.2 OPTIMUM RECEIVER--DETECTION SENSITIVITY INDEX, d'

Given an object to be detected in the presence of a specific type of noise, the best detection performance that is possible may be determined through application of signal detection theory (Whalen, 1971; Van Trees, 1968; Wagner, 1978). The best decision criterion that can be used in a given detection problem is referred to as the "optimum receiver" in signal detection theory. The optimum

receiver will depend on the situation at hand. In particular, the optimum receiver must take into account the properties of the noise to be "optimum." It is often possible to characterize the detection performance of the optimum receiver without actually constructing or implementing the detection criterion.

The detection performance of any detector applied to a given detection task may be summarized by its receiver operating characteristic (ROC) curve. The ROC curve is a plot of the probablity of a "true positive" response versus the probability of a "false positive" response (Chapter 115; Green and Swets, 1966). For additive, Gaussian distributed noise, the ROC curve for the binary decision problem may be completely specified by a single parameter, sensitivity index d'. The d' depends on the object's contrast, size, and shape as well as on the magnitude and correlations of the noise. For the optimum receiver d' may be expressed in terms of the frequency representation of the object R(f) as follows (Bernard, 1972)

$$d'_{OPTIMUM} = \int df_x df_y \frac{|R(f)|^2}{S(f)} \quad (4)$$

where S is the noise power spectrum (see earlier discussion of dependence on reconstruction algoritnm and NEQ). It is observed that $d'_{OPTIMUM}$ is determined by the frequency sum or integral of the ratio of the signal power to the noise power. It should be noted that the design of an optimum receiver depends critically on the properties of the noise. Thus a receiver that is optimum for white (uncorrelated) noise will not be optimum for CT noise.

The plausibility of equation 4 may be illustrated for two limiting cases. For the first case the following situation will be considered: S is zero for some finite frequency interval in which the object power $|R|^2$ is not zero. The integrand in equation 4 would then be infinite over that frequency interval yielding an infinite value for $d'_{OPTIMUM}$. This is reasonable, since the optimum receiver would only have to check the image power (after the known background was removed) in the appropriate frequency interval. If there was any power present, it could only be due to the object. The optimum receiver could never make a mistake! Hence, $d'_{OPTIMUM} = \infty$. In the second case, the situation in which $|R|^2$ is zero over some finite frequency interval is considered. Equation 4 indicates that noise power in that frequency interval will not influence the optimim receiver. Again, this is reasonable, since the optimum receiver can remove these frequency intervals from consideration by Fourier transformation of the image followed by zeroing out the Fourier amplitudes in the relevant frequency interval.

Equation 4 leads one to an interesting conclusion concerning the trade-off between noise magnitude and spatial resolution. It is well known that the rms noise may be reduced by smoothing the image. Smoothing also results in a loss of spatial resolution, which is supposed to make it more difficult to detect small objects or to locate the positions of sharp edges. However, image smoothing is equivalent to the multiplication of the frequency representation of the image by a filter, which generally reduces the high frequency components of the image. Since both $|R|^2$ and S are affected by the filter in the same way, equation 4 indicates that $d'_{OPTIMUM}$ is not altered by the smoothing process, unless the filter is zero for some finite range of frequencies where $|R|^2$ is not zero. Thus, the performance of the optimum receiver is not affected by smoothing (unless information is lost by a zero filter). Indeed, it is not necessary to trade off between low noise and high spatial resolution for the optimum receiver.

These statements concerning the optimum receiver may or may not have bearing on what might be expected of a human observer. For example, the human observer may suffer critical band masking between frequency intervals. Thus, it is unlikely that the human observer could make use of information in one frequency interval that through filtering was reduced by a factor 100 relative to neighboring frequency intervals. The "optimum receiver," being a conceptual entity, would have no difficulty recouping the information in the attenuated frequency band.

Although the optimum receiver may not realistically characterize the performance of the human observer, it provides the ultimate standard against which the human observer may be compared. If it is found that the performance of the human observer falls short of this ideal in the simple detection task envisioned, then it may prove useful to explore the reasons for the shortcomings of the human observer.

3.3 APPLICATION TO CT

The application of signal detection theory to computed tomography leads to an interesting result concerning the transfer of detection information from the projections to the reconstruction (Hanson, 1979a). The projection data themselves may be used to detect the presence of an object within the projection field. It is found that when the totality of projection data is analyzed by the optimum receiver, the resulting $d'_{OPTIMUM}$ is equal to or greater than the $d'_{OPTIMUM}$ obtained from analysis of the reconstruction. In other words, the detection in a CT reconstruction of a specific object on a known background can be no better than when the detection of the same object is based on the direct projection measurements. Furthermore, the detection performance based on an efficient reconstruction can equal that based on the projections. It has been shown that the filtered back projection algorithm is efficient, in this sense, for the detection of large objects (Hanson, 1979a, 1980). In the practical case of reconstruction in a discrete pixel array from discretely sampled projections, there can be a loss of information leading to some degradation in detection sensitivity (Hanson, 1979b).

The frequency representation R(f) of an object with large area is concentrated at low frequencies. Then equation 4 indicates that the detection sensitivity of large-area objects will principally be determined by the low-frequency content of the noise power. Since statical CT noise has a ramplike noise power spectrum at low frequencies, the single parameter that characterizes the slope of the ramp NEQ is a sufficient measure of the detection sensitivity for large objects. It is found (Hanson, 1979a) that the optimum sensitivity index is

$$d'_{OPTIMUM} = \Delta\mu\, A^{1/4}\, NEQ \quad . \qquad (5)$$

where $\Delta\mu$ is the average contrast of the object with an effective area A. Equation 5 is a good approximation for most objects of large area (square, circle, etc.). This result establishes the intimate connection between NEQ and the detectability of large-area objects. The $A^{1/4}$ dependence of $d'_{OPTIMUM}$ should be noted. It arises from the ramplike nature of the CT noise power spectrum. For white noise (β = constant), d' is proportional to $A^{1/2}$.

3.4 HUMAN OBSERVER

The relationship between the detection capabilities of the ideal detector and those of the human observer has not been fully explored for images containing CT noise. Judy et al. (1981) have found that human observer's performance does follow that of an ideal observer when the size and contrast of the object to be detected is varied. It is possible that human observers may have shortcommings, particularly in their ability to integrate the noise over the object area. The unusual correlations present in CT reconstruction may prove difficult for the eye-brain to take into account. Several psychophysical studies (Hanson, 1977; Joseph, 1977, 1978; Chew et al., 1978; Orphanoudakis, 1981) have shown that under certain circumstances observer detectability of large objects is improved by smoothing CT images. The reason for this improvement remains to be explained. Furthermore, the $A^{1/4}$ dependence in the threshold contrast for a constant d' predicted in equation 5 has not been verified for human observers (Cohen, 1979; Cohen and DiBianca, 1979). The effects of altered viewing conditions and training have yet to be investigated.

3.5 THREE-DIMENSIONAL ASPECTS

The discussion of preceding sections dealt with the detection of a two-dimensional object in a single CT scan. In reality, however, the radiologic detection problems are three dimensional in nature. The difficulties in detecting three-dimensional objects in CT scans are often referred to as "partial volume" effects. To illustrate the problem, consider the detection of a sphere of diameter d immersed in a uniform background of slightly lower density. If the sphere happened to lie completely within a single CT slice, its effective reconstruction density would be less than its actual density because of the partial volume effect. But, if adjacent slices happened to split the sphere in half, its reconstructed density would be halved relative to the case just described. In the latter situation, the detection of the sphere is made more difficult by the large reduction in its reconstruction density, particularly if each slice is viewed independently. An improvement in detection could be attained by simply averaging the two slices, since the rms noise would be reduced by a factor of

$2^{-1/2}$. This problem illustrates the desirability of a display system that allows full use of the three-dimensional information available in CT (Hanson, 1979a).

4. CONCLUSION

The detection limitations inherent in statistically limited computed tomographic (CT) images have been described through the application of signal detection theory. The detectability of large-area, low-contrast objects has been shown to be chiefly dependent on the low-frequency content of the noise power spectral density. For projection data containing uncorrelated noise, the resulting ramplike, low-frequency behavior of the noise power spectrum of the CT reconstruction may be conveniently characterized by the density of noise-equivalent quanta (NEQ) detected in the projection measurements. The NEQ for a given image can be determined from a measurement of the noise power spectrum. The detection of large objects is as good in an efficient reconstruction (e.g., filtered back projection) as that based on the projection data.

5. REFERENCES

Barnes, G. T., Yester, M. V., and King, M. A., Optimizing Computed Tomography (CT) Scanner Geometry, Proc. SPIE Appl. Opt. Instr. in Medicine VII 173, pp. 225-237, 1979.

Barrett, H. H., Gordon, S. K., and Hershel, R. S., Statistical Limitations in Transaxial Tomography, Comput. Biol. Med. 6, pp. 307-323, 1976.

Brooks, R. A., and Di Chiro, G., Statistical Limitations in X-ray Reconstructive Tomography, Med. Phys. 3, pp. 237-240, 1976.

Chester, D. A. Riederer, S. J., and Pelc, J. J., Noise due to Photon Counting Statistics in Computed X-ray Tomography, J. Comput. Assist. Tomogr. 1, pp. 64-74, 1977.

Chew, E., Weiss, G. H., Brooks, R. A., and Di Chiro, G., Effect of CT Noise on Detectability of Test Objects, Am. J. Roentgenol. 131, pp. 681-685, 1978.

Cho, Z. H., Chan J. K., Hall, E. L., Kruger, R. P., and McCaughey, D. G., A Comparative Study of 3-D Image Reconstruction Algorithms with Reference to Number of Projections and Noise Filtering, IEEE Trans. Nucl. Sci. NS-22, pp. 344-358, 1975.

Cohen, G., Contrast-detail-dose Analysis of Six Different Computed Tomographic Scanners, J. Comput. Assist. Tomogr. 3, pp. 197-203, 1979.

Cohen, G., and DiBianca, F. A., The Use of Contrast-detail-dose Evaluation of Image Quality in a Computed Tomographic Scanner, J. Comput. Assist. Tomogr. 3, pp. 189-195, 1979.

Dainty, J. C., and Shaw, R., Image Science; Principles, Analysis and Evaluation of Photographic-type Imaging Processes, London, 1974, Academic Press, Inc. Ltd.

Goodenough, D. J., Objective Measures Related to ROC Curves, Proc. SPIE Appl. Opt. Instr. in Medicine III 47, pp. 134-141, 1975.

Goodenough, D. J. and Metz, C. E., Effects of Listening Interval on Auditory Detection Performance, J. Acoust. Soc. Am. 55, pp. 111-116, 1974.

Green, D. M., and Swets, J. A., Signal Detection Theory and Psychophysics, New York, 1966, John Wiley & Sons, Inc.

Hanson, K. M., Detectability in the Presence of Computed Tomographic Reconstruction Noise, Proc. SPIE Appl. Opt. Instr. in Medicine VI 127, pp. 304-312, 1977.

Hanson, K. M. and Boyd, D. P., The Characteristics of Computed Tomographic Reconstruction Noise and their Effect on Detectability., IEEE Trans. Nucl. Sci., NS-25, pp. 160-173, 1978.

Hanson, K. M., Detectability in Computed Tomographic Images, Med. Phys. 6, pp. 441-451, 1979a.

Hanson, K. M., The Detective Quantum Efficiency of CT Reconstruction: The Detection of Small Objects., Proc. SPIE Appl. Opt. Instr. in Medicine VII 173, pp. 291-298, 1979b.

Hanson, K. M., On the Optimality of the Filtered Backprojection Algorithm, J. Comput. Assist. Tomogr. 4, pp. 361-363, 1980.

Hanson, K. M, Noise and Contrast Discrimination in Computed Tomography, in Radiology of the Skull and Brain, ed. Newton, T. H. and Potts, D. G., Vol. 5, pp. 3941-3955, 1981.

Herman, G. T., On the Noise in Images Produced by Computed Tomography, Tech. Report No. MIPG33, Suny Buffalo, 1979.

Huesman, R. H., Analysis of Statistical Errors for Transverse Section Reconstruction, Lawrence Berkeley Laboratory Report #4278, 1975, University of California, Berkeley, CA.

Huesman, R. H., The Effects of a Finite Number of Projection Angles and Finite Lateral Sampling of Projections on the

Propagation of Statistical Errors in Transverse Section Reconstruction, Phys. Med. Biol. 22, pp. 511-521, 1977.

Johns, H. E., and Cunningham, J. R., The Physics of Radiology, Ed. 3, Springfield, 1969, Charles C. Thomas.

Joseph, P. M., Image Noise and Smoothing in Computed Tomography (CT) Scanners, Proc. SPIE Appl. Opt. Instr. in Medicine VI, 127, pp. 396-399, 1978.

Joseph, P. M., Artifacts in Computed Tomography, in Radiology of the Skull and Brain, ed. Newton, T. H. and Potts, D. G., Vol. 5, pp. 3956-3992, 1981.

Judy, P. F., Swensson, R. G., and Szulc, M., Legion Detection and Signal-to-noise Ratio in CT Images, Med. Phys. 8, pp. 13-23, 1981.

New, P. F. J., Scott, W. R. Schnur, J. A. Davis, F. R., and Taveras, J. M., Computerized Axial Tomography with the EMI Scanner, Radiology 110, pp. 109-123, 1973.

Orphanoudakis, S. C., Hirsch, J., Jaffe, C. C., and Rauschkolb, E., "Receiver Operating Characteristic Analysis of Observer Performance in Computed Tomography," submitted to Radiology, 1981.

Riederer, S. J., Pelc, N. J., and Chesler, D. A., The Noise Power Spectrum in Computed X-ray Tomography, Phys. Med. Biol. 23, pp. 446-454, 1978.

Shepp, L. A., and Logan, B. F., The Fourier REconstruction of a Head Section, IEEE Trans. Nucl. Sci. NS-21, pp. 21-43, 1974.

Tanaka, E., and Iinuma, T. A., Corrective Functions for Optimizing the Reconstructed Image in Transverse Section Scan, Phys. Med. Biol. 20, pp. 789-798, 1975.

Tanaka, E., and Iinuma, T. A., Corrective Functions and Statistical Noises in Transverse Section Picture Reconstruction, Comput, Biol. Med. 6, pp. 295-306, 1976.

Van Trees, H. L., Detection, Estimation and Modulation Theory, New York, 1968, John Wiley & Sons, Inc.

Wagner, R. F., Fast Fourier Digital Quantum Mottle Analysis with Application to Rare Earth Intensifying Screen Systems, Med. Phys. 4, pp. 157-162, 1976.

Wagner, R. F., Toward a Unified View of Radiological Imaging Systems. II. Noisy Images, Med. Phys. 4, pp. 279-296, 1977.

Wagner, R. F., Decision Theory and the Detail Signal-to-noise Ratio of Otto Schade, Photogr. Sci. Eng. 22, pp. 41-46, 1978

Wagner, R. F., Brown, D. G., and Pastel, M. S., The Application of Information Theory to the Assessment of Computed Tomography, Med. Phys. 6, pp. 83-94, 1979.

Whalen, A. D., Detection of Signals in Noise, New York, 1971 Academic Press, Inc.

Fig. 1 Three scans of a contrast sensitivity phantom taken on a GE CT/T 7800 scanner at two exposures: 1152 MAS (top) and 307 MAS (bottom). Higher dose leads to lower noise and improved contrast sensitivity. (Courtesy of F. A. DiBianca, General Electric).

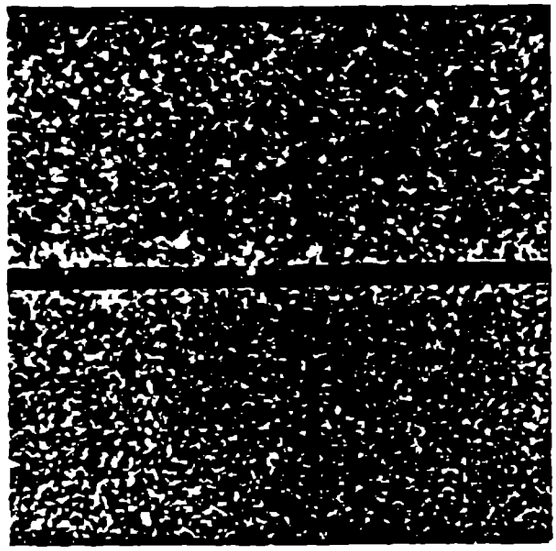

Fig. 2 Comparison of "white" noise (top) and CT noise (bottom) each with the same rms deviation. The lack of low-frequency structure in the CT noise is evident especially when viewed at a distance.

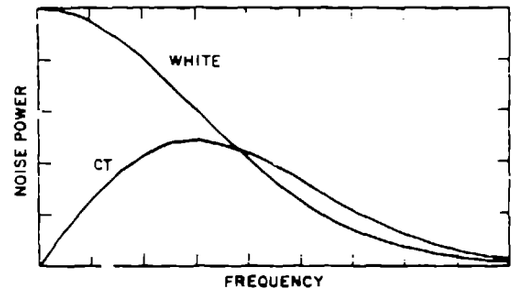

Fig. 3 Noise power spectrum of the two images in Fig. 2.

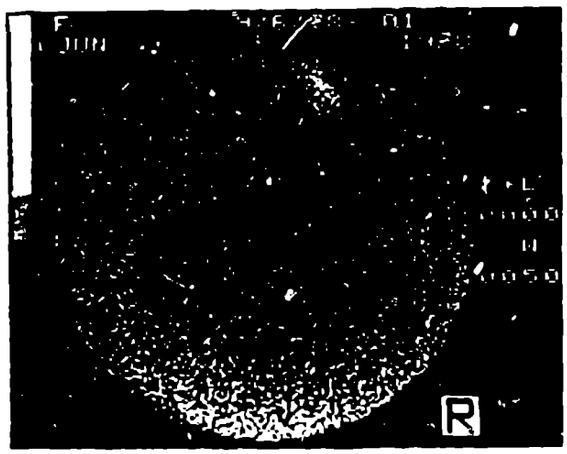

Fig. 4 EMI CT-5005 scan of the EMI water phantom used in calculation of noise power spectrum. The light spot near the top of the reconstruction is a roller mark produced by the film processing unit. (Courtesy D. P. Boyd, Univeristy of California, San Francisco.)

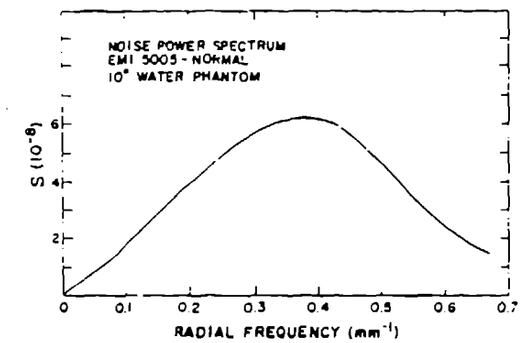

Fig. 5 Noise power spectrum for normal 20-sec scans on an EMI CT-5005 of a 24-cm-diameter water phantom. The slope of the spectrum at low frequencies determines NEQ.